J|A|C|S
ARTICLES
Published on Web 01/17/2007

9-Donor-Substituted Acridizinium Salts: Versatile Environment-Sensitive Fluorophores for the Detection of Biomacromolecules

Anton Granzhan,[†,§] Heiko Ihmels,*[,†] and Giampietro Viola[‡]

Contribution from the University of Siegen, Organic Chemistry II, Adolf-Reichwein-Strasse 2, D-57068 Siegen, Germany, and Department of Pharmaceutical Sciences, University of Padova, via Marzolo 5, 35131 I-Padova, Italy

Received September 25, 2006; E-mail: ihmels@chemie.uni-siegen.de

Abstract: The absorption and steady-state emission properties of a series of *N*-alkyl- and *N*-aryl-9-aminoacridizinium derivatives and two 9-sulfanyl-substituted acridizinium derivatives were investigated. The *N*-alkyl derivatives and the 9-methylsulfanylacridizinium have an intense intrinsic fluorescence (φ_f = 0.2−0.6), whereas the *N*-aryl-substituted compounds are virtually nonfluorescent in liquid solutions ($\varphi_f \leq$ 0.01). The emission intensity of the latter compounds significantly increases with increasing viscosity of the medium. It is demonstrated that the excited-state deactivation of the *N*-aryl-9-aminoacridizinium derivatives is due to two nonradiative processes: (i) torsional relaxation by rotation about the N−aryl bond and (ii) an electron-transfer process from an electron-donor substituted phenyl ring to the photoexcited acridizinium chromophore. The binding of several representative acridizinium derivatives to double-stranded DNA was studied by the spectrophotometric titrations and linear dichroism spectroscopy. The results give evidence that the prevailing binding mode is intercalation with binding constants in the range (0.5−5.0) × 10^5 M^{-1} (in base pairs). Notably, the binding of most of the *N*-aryl-9-aminoacridizinium derivatives leads to a fluorescence enhancement by a factor of up to 50 upon binding to the biomacromolecules. Moreover, the addition of selected proteins, namely albumins, to *N*-(halogenophenyl)-9-aminoacridizinium ions in the presence of an anionic surfactant (sodium dodecyl sulfate) results in a 20-fold fluorescence enhancement. In each case, the emission enhancement is supposed to result from the hindrance of the torsional relaxation in the corresponding binding site of the biomacromolecule, which in turn suppresses the excited-state deactivation pathway.

Introduction

Fluorescent probes are valuable tools in chemistry, materials science, biology, and medicine, mainly because of the high sensitivity of fluorescence spectroscopy.[1,2] While the use of fluorescent nanoparticles and supramolecular conjugated dendrimers offers distinct advantages, such as enhanced photopersistence and high luminescence quantum yields in combination with large extinction coefficients,[3] small organic dye molecules and luminescent complexes of transition metals with organic ligands offer the opportunity to vary the chemical and photophysical properties of fluorescent probes by a deliberate choice of the fluorophore and a systematic variation of the substitution pattern and, thus, provide an access to an almost unlimited range of possible applications.[4]

In particular, fluorescent probes whose emission intensity increases upon association with biomacromolecules, such as DNA or proteins, are useful markers in genomics and proteomics, because the binding event to the host molecule may be followed by the appearance of an intense fluorescence emission ("light-up probes").[5] Their major applications are staining of nucleic acids and proteins in gel electrophoresis and the quantification of these biomacromolecules.[6−8] Thus, efficient

[†] University of Siegen.
[‡] University of Padova.
[§] Present address: Laboratoire de chimie des interactions moléculaires, Collège de France, Paris, France.

(1) (a) *Optical Sensors*; Wolfbeis, O. S., Ed.; Springer-Verlag: Heidelberg, 2004. (b) Mohr, G. J. *Chem.—Eur. J.* **2004**, *10*, 1082−1090. (c) Pu, L. *Chem. Rev.* **2004**, *104*, 1687−1716. (d) Martinez-Manez, R.; Sancenon, F. *Chem. Rev.* **2003**, *103*, 4419−4476. (e) Valeur, B. *Molecular Fluorescence: Principles and Applications*; Wiley-VCH: Weinheim, 2002. (f) Wiskur, S. L.; Ait-Haddou, H.; Anslyn, E. V.; Lavigne, J. J. *Acc. Chem. Res.* **2001**, *34*, 963−972. (g) de Silva, A. P. H.; Gunaratne, Q.; Gunnlaugsson, T.; Huxley, A. J. M.; McCoy, C. P.; Rademacher, J. T.; Rice, T. E. *Chem. Rev.* **1997**, *97*, 1515−1566.
(2) Wahl, M.; Koberling, F.; Patting, M.; Rahn, E. H. *Curr. Pharm. Biotechnol.* **2004**, *5*, 299−308.
(3) (a) Rosi, N. L.; Mirkin, C. A. *Chem. Rev.* **2005**, *105*, 1547−1562. (b) Grimsdale, A. C.; Müllen, K. *Angew. Chem.* **2005**, *117*, 5732−5772. *Angew. Chem., Int. Ed.* **2005**, *44*, 5592−5629. (c) Mongin, O.; Rama Krishna, T.; Werts, M. H. V.; Caminade, A.-M.; Majoral, J.-P.; Blanchard-Desce, M. *Chem. Commun.* **2006**, 915−917. (d) Sapsford, K. E.; Berti, L.; Medintz, I. L. *Angew. Chem.* **2006**, *118*, *4676*−4704; *Angew. Chem., Int. Ed.* **2006**, *45*, 4562−4588.
(4) Haugland, R. G. *Handbook of Fluorescent Probes and Research Products*, 9th ed.; 2002.
(5) Prentø, P. *Biotech. Histochem.* **2001**, *76*, 137−161.
(6) (a) Jin, L.-T.; Choi, J.-K. *Electrophoresis* **2004**, *25*, 2429−2438. (b) Williams, L. R. *Biotech. Histochem.* **2001**, *76*, 127−132.
(7) Cosa, G.; Focsaneanu, K.-S.; McLean, J. R. N.; McNamee, J. P.; Scaniano, J. C. *Photochem. Photobiol.* **2001**, *73*, 585−599.
(8) (a) Herr, A. E.; Singh, A. K. *Anal. Chem.* **2004**, *76*, 4727−4733. (b) Giordano, B. C.; Jin, L.; Couch, A. J.; Ferrance, J. P.; Landers, J. P. *Anal. Chem.* **2004**, *76*, 4705−4714.

10.1021/ja0668872 CCC: $37.00

probes for the fluorimetric detection of DNA are available, including numerous organic dyes[4] and several luminescent ruthenium complexes.[9] The fluorescent protein stains include, among others, 1-anilino-8-naphthalenesulfonate (1,8-ANS),[10] Nile Red,[11] or the SYPRO dye family.[12] Nevertheless, studies aimed at a better understanding of the origin of the fluorescence properties of a given fluorophore, in particular the dependence on the environment, are scarcely addressed in the literature. The mechanism of the DNA-induced fluorescence enhancement of ruthenium-based metallointercalators has been investigated in detail;[9b,c] however, the situation is less clear in the case of DNA-sensitive organic fluorophores, in particular due to their vast structural diversity. For example, the mechanism of the fluorescence enhancement of ethidium bromide upon binding to DNA has been a matter of debate for more than 20 years.[13,14] Even less investigated is the mechanism of protein detection by light-up probes. Especially in the latter case, the discovery of novel efficient fluorescent probes rests mainly on serendipitous findings[15] and only few systematic strategies for the *rational design* of light-up probes or detailed analyses of structure−property relationships are published.[16]

Previous studies from our groups have shown that derivatives of the acridizinium (benzo[*b*]quinolizinium) ion represent a promising platform for DNA-binding compounds.[17] Along these lines, the 9-aminoacridizinium (**1**)[18] represents a system with attractive photophysical properties, such as absorption in the near-UV region of the spectrum ($\lambda_{max} \approx 390$ nm), well separated from the one of the nucleic bases; good quantum yield of fluorescence ($\varphi_f = 0.41$ in aqueous solutions);[19] and a large Stokes shift ($\Delta\lambda \approx 120$ nm), allowing unambiguous detection without reabsorption effects and not interfering with the background fluorescence of biomolecules. However, upon interaction with the DNA bases, the fluorescence of **1** is significantly quenched due to the photoinduced electron-transfer reaction with the nucleic bases which is a major drawback with respect to its use as a light-up probe.[20] Therefore, we planned to modify the structure of **1** (Chart 1) in such a way that it has a very low intrinsic fluorescence, which may increase upon complex formation with DNA or other biomacromolecules.

Chart 1. Structures Investigated and Discussed in This Study[a]

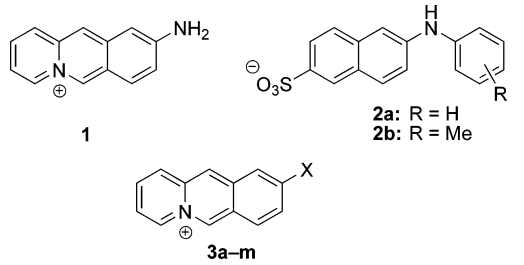

[a] Assignment of substituents X, see Table 1.

To impair the intrinsic fluorescence properties of **1**, an additional deactivation pathway for the excited state was planned to be introduced by an aryl substituent at the exocyclic nitrogen atom, which may result in two effects: (i) a photoinduced electron-transfer reaction between the electron-rich phenyl substituent and the excited acridizinium chromophore; (ii) rotation about the N−aryl bond, leading to the nonradiative deactivation of the excited state. For comparison, it has been shown that in protein stains such as 2-anilino-6-naphthalenesulfonate derivatives (**2a**: ANS; **2b**: TNS)[10] both effects take place.[21] Similarly, the binding of *N*-aryl-9-aminoacridizinium derivatives to a host molecule may hinder one or both of the deactivation pathways, resulting in an increase of the fluorescence signal. Moreover, the use of the novel acridizinium-based chromophore has advantages compared to compounds **2**, because the positively charged acridizinium chromophore provides appropriate DNA-binding properties. In addition, binding to the negatively charged protein−surfactant micelles in the presence of an anionic surfactant, e.g., SDS, which is used in the gel electrophoresis of proteins,[6,22] may be possible and provide a tool for the visualization of proteins after gel electrophoresis.

Since the photophysical properties of intramolecular donor−acceptor systems, such as **2**, are often influenced by several independent effects, their detailed investigation represents a challenging research field[21] and a systematic study is desirable. This, in part, may be achieved by the synthesis and detailed investigation of a series of derivatives with different substituents in the phenyl ring, such as electron-donating, electron-withdrawing, or halogen substituents. Moreover, the substitution pattern may be varied, too. This approach would allow the deduction of a structure−properties relationship and, as a final goal, tuning the photophysical properties of the system in such a way that it could match a particular practical application.

To obtain insight into the photophysical properties of the 9-aminoacridizinium system in general, a study of the derivatives with substituents other than aryl groups was also planned. Thus, *N*-alkyl- or *N*,*N*-dialkyl-substituted derivatives of **1** appeared to be useful in studying the electron-donating effect of the alkyl

(9) (a) Friedman, A. E.; Chambron, J.-C.; Sauvage, J.-P.; Turro, N. J.; Barton, J. K. *J. Am. Chem. Soc.* **1990**, *112*, 4960−4962. (b) Hiort, C.; Lincoln, P.; Nordén, B. *J. Am. Chem. Soc.* **1993**, *115*, 3448−3454. (c) Olson, E. J. C.; Hu, D.; Hörmann, A.; Jonkman, A. M.; Arkin, M. R.; Stemp, E. D. A.; Barton, J. K.; Barbara, P. F. *J. Am. Chem. Soc.* **1997**, *119*, 11458−11467. (d) Erkkila, K. E.; Odom, D. T.; Barton, J. K. *Chem. Rev.* **1999**, *99*, 2777−2795.
(10) (a) Hartman, B. K.; Udenfriend, S. *Anal. Biochem.* **1969**, *30*, 391−394. (b) Horowitz, P. M.; Bowman, S. *Anal. Biochem.* **1987**, *165*, 430−434. (c) Edelman, G. O.; McClure, W. O. *Acc. Chem. Res.* **1968**, *1*, 65−70.
(11) Daban, J.-R.; Bartolomé, S.; Samsó, M. *Anal. Biochem.* **1991**, *199*, 169−174.
(12) (a) Berggren, K.; Chernokalskya, E.; Steinberg, T. H.; Kemper, C.; Lopez, M. F.; Diwu, Z.; Haugland, R. P.; Patton, W. F. *Electrophoresis* **2000**, *21*, 2509−2521. (b) Steinberg, T. H.; Jones, L. J.; Haugland, R. P.; Singer, V. L. *Anal. Biochem.* **1996**, *239*, 223−237.
(13) (a) Olmsted, J., III; Kearns, D. R. *Biochemistry* **1977**, *16*, 3647−3654. (b) Löber, G. *J. Lumin.* **1981**, *22*, 221−265. (c) Sailer, B. L.; Nastasi, A. J.; Valdez, J. G.; Steinkamp, J. A.; Crissman, H. A. *J. Histochem. Cytochem.* **1997**, *45*, 165−175. (d) Sailer, B. L.; Nastasi, A. J.; Valdez, J. G.; Steinkamp, J. A.; Crissman, H. A. *Cytometry* **1996**, *25*, 164−172. (e) Heller, D. P.; Greenstock, C. L. *Biophys. Chem.* **1994**, *50*, 305−312.
(14) Luedtke, N.; Liu, Q.; Tor, Y. *Chem.−Eur. J.* **2005**, *11*, 495−508.
(15) (a) Jisha, V. S.; Arun, K. T.; Hariharan, M.; Ramaiah, D. *J. Am. Chem. Soc.* **2006**, *128*, 6024−6025. (b) Daban, J. R.; Bartolome, S.; Samso, M. *Anal. Biochem.* **1991**, *199*, 169−174. (c) Lee, S. H.; Suh, J. K.; Li, M. *Bull. Korean Chem. Soc.* **2003**, *24*, 45−48.
(16) (a) Patonay, G.; Salon, J.; Sowell, J.; Strekowski, L. *Molecules* **2004**, *9*, 40−49. (b) Rabilloud, T.; Strub, J.-M.; Luche, S.; Girardet, J. L.; van Dorsselaer, A.; Lunardi, J. l. *Proteome* **2000**, *1*, 1−14. (c) Rodembusch, F. S.; Leusin, F. P.; Medina, L. F. D.; Brandelli, A.; Stefani, V. *Photochem. Photobiol. Sci.* **2005**, *4*, 254−259.
(17) Ihmels, H.; Faulhaber, K.; Sturm, C.; Bringmann, G.; Messer, K.; Gabellini, N.; Vedaldi, D.; Viola, G. *Photochem. Photobiol.* **2001**, *74*, 505−511.
(18) Ihmels, H.; Engels, B.; Faulhaber, K.; Lennartz, C. *Chem.−Eur. J.* **2000**, *6*, 2854−2864.
(19) In ref 18, a value of $\varphi_f = 0.12$ in water for compound **1** has been given. However, further experiments revealed that this value was under-estimated due to the use of an inappropriate quantum yield standard (quinine). The values in the present work were determined using Coumarin 153 as a reference and are believed to be more reliable.
(20) Bohne, C.; Faulhaber, K.; Giese, B.; Häfner, A.; Hofmann, A.; Ihmels, H.; Köhler, A.-K.; Perä, S.; Schneider, F.; Sheepwash, M. A. L. *J. Am. Chem. Soc.* **2005**, *126*, 76−85.
(21) Kosower, E. M. *Acc. Chem. Res.* **1982**, *15*, 259−266.
(22) Osterman, L. A. *Methods of Protein and Nucleic Acid Research;* Springer: Berlin, 1984.

groups on the 9-aminoacridizinium chromophore and, on the other hand, serving as reference compounds for the investigation of the effects of the aryl substituent. Finally, investigation of a sulfur analogue of **1** was planned, in which the amino group is replaced with a sulfanyl or phenylsulfanyl substituent. Since the sulfanyl substituent has different electron-donating properties than the amino substituent in **1**, it was proposed that such derivatives could represent a complementary donor−acceptor system.

Results

Photophysical Properties. A. Absorption and Fluorescence Properties of 9-Amino-substitued Derivatives. Compounds **3a**−**k** were synthesized by aromatic cyclodehydration or nucleophilic aromatic substitution.[23] The acridizinium salts are well-soluble in protic and polar aprotic solvents and moderately soluble in halogenated solvents, such as dichloromethane and chloroform (except for **1**). Unfortunately, the solubility of these compounds in the solvents of moderate polarity (1,4-dioxane, ethyl acetate) is lower than that required for UV/vis spectroscopy which excludes investigations therein. The diluted solutions of all investigated compounds are yellow. Representative absorption and emission spectra of selected 9-amino-substituted acridizinium derivatives are shown in Figure 1; photophysical parameters of the new compounds from spectrophotometric and spectrofluorimetric measurements in aqueous solutions are given in Table 1. The complete set of data on the absorption and fluorescence properties of compounds **1** and **3a**−**m** in various solvents is presented in Table S1 (Supporting Information).

The most remarkable feature of the absorption spectra is the close similarity of the positions and shapes of absorption bands of all 9-aminoacridizinium derivatives. Thus, the introduction of aryl substituents (**3d**−**k**) into the 9-aminoacridizinium framework does not result in significant changes in the absorption spectra as compared to the dialkyl-substituted derivatives **3a**−**b**. At the same time, the absorption spectra of all amino-substituted derivatives (**3a**−**k**) are red-shifted by 9−15 nm with respect to the parent compound **1**. Moreover, the shape of the long-wavelength absorption band of the aryl-substituted compounds **3f**−**k** is essentially identical (Figure 1C and D). Notably, absorption spectra of the derivatives with electron-donating substituents in the phenyl ring (**3d**, **3e**) are slightly broadened as compared to the derivatives **3f**−**k**, although the positions of the long-wavelength maxima do not change significantly in this case, either (Figure 1B). This broadening is more pronounced in aprotic solvents, such as DMSO and halogenated solvents. The absorption spectra of compound **3d** were investigated in a broad range of concentrations (0.01−1 mM in dichloromethane); however, it was observed that the shape of the absorption spectrum remains unchanged within this concentration range (Figure S1A; Supporting Information).

Acridizinium derivatives **1** and **3a**−**k** exhibit only weak solvatochromism. The photophysical properties of two representative derivatives **3b** and **3k** in various solvents are displayed in Table 2. Thus, the absorption maxima of all compounds are most red-shifted in dichloromethane (e.g., for **3k**: the absorption maximum $\lambda_{abs} = 413$ nm in dichloromethane vs 397 nm in water and acetonitrile; see also Table S1, Supporting Information).

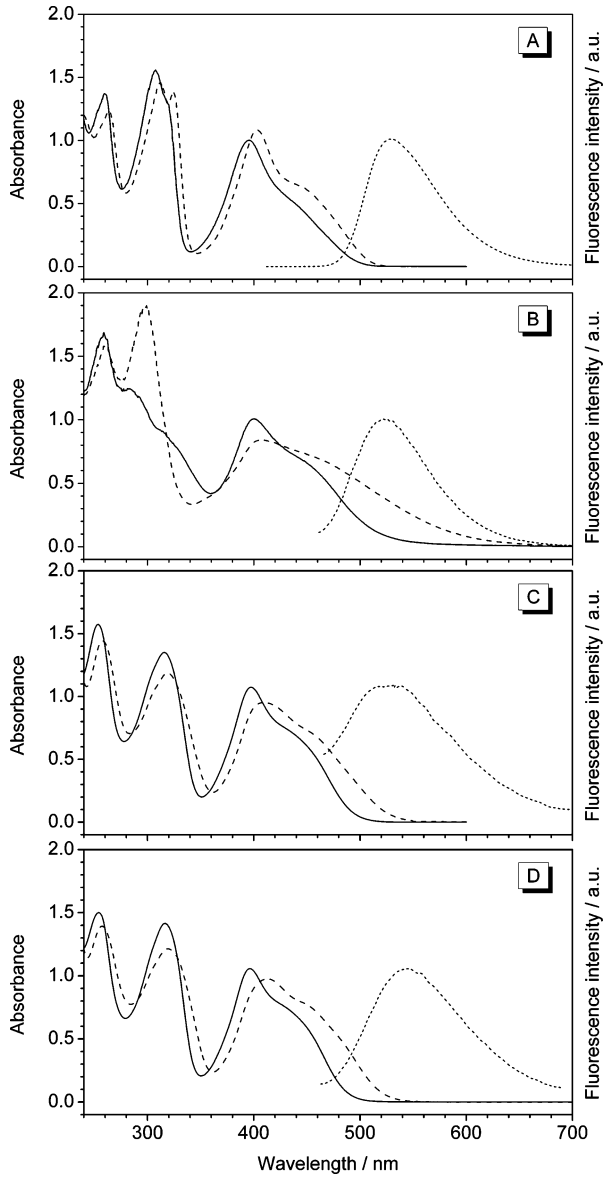

Figure 1. Absorption and fluorescence spectra of compounds **3a** (A), **3d** (B), **3g** (C), and **3k** (D). Solid lines: absorption spectra in water; dashed lines: absorption spectra in dichloromethane, $c = 50$ μM in both cases. Dotted lines: normalized fluorescence emission spectra in water, $c = 10$ μM, excitation wavelength $\lambda_{exc} = 390$ nm.

In the other solvents investigated (water, methanol, acetonitrile, DMSO, chloroform), only minor shifts (8 nm at maximum) of the absorption maxima were observed.

The solutions of the dialkylamino-substituted derivatives **3a**−**c** exhibit a characteristic, bright yellow-green fluorescence similar to the one of the parent 9-aminoacridizinium salt **1**.[18] The fluorescence quantum yield in dichloromethane ($\varphi_f \approx 0.5$−0.6; cf. Table S1, Supporting Information) is almost twice as high as in other solvents (e.g., for **3a** $\varphi_f = 0.36$ both in methanol and acetonitrile). The emission spectra of these derivatives have a maximum at 525−540 nm, depending on the solvent, and a large Stokes shift (120−140 nm) is observed. The Stokes shift values are smallest in dichloromethane.

In contrast to compounds **3a**−**c**, the arylamino-substituted derivatives **3d**−**k** exhibit very weak fluorescence in various solvents, usually just slightly exceeding the detection limit of the instrument ($\varphi_f \geq 1 \times 10^{-4}$). In some cases, the fluorescence

(23) (a) Granzhan, A.; Ihmels, H. *Org. Lett.* **2005**, *7*, 5119−5122. (b) Granzhan, A.; Ihmels, H. *ARKIVOC* **2007**, (*viii*), 136−149.

Table 1. Spectrophotometric Properties of Acridizinium Derivatives **1** and **3a**−**m** in Water

compd	X	λ_{abs}[a]/ nm	log ϵ/ cm^{-1} M^{-1} [b]	λ_{em}[c]/ nm	$\varphi_f \times 10^2$ [d]
1	NH_2	387	4.26	512	41
3a	$N(CH_2CH_2)_2O$	396	4.30	528	40
3b	$N(CH_2)_4$	404	4.33	535	36
3c	NEt_2	404	4.31	532	17
3d	$NH(4\text{-}C_6H_4NMe_2)$	400	4.30	523	0.21
3d-H^+		397	4.34	523	0.38
3e	$NH(4\text{-}C_6H_4OMe)$	399	4.28	530	0.02
3f	$NH(4\text{-}C_6H_4Me)$	399	4.35	*e*	*e*
3g	NHPh	398	4.33	526	0.01
3h	$NH(4\text{-}C_6H_4F)$	396	4.34	545	0.01
3i	$NH(4\text{-}C_6H_4Br)$	398	4.33	550	0.01
3j	$NH(4\text{-}C_6H_4Cl)$	397	4.32	513	0.07
3k	$NH(3\text{-}C_6H_4Cl)$	397	4.33	550	0.08
3l	SPh	390	4.24	475	0.04
3m	SMe	389	4.17	493	21

[a] Long-wavelength absorption maxima, $c = 50$ μM. [b] Molar decadic absorption coefficient. [c] Fluorescence emission maximum, $c = 10$ μM, excitation wavelength $\lambda_{ex} = 390$ nm. [d] Fluorescence quantum yield (relative to Coumarin 153, estimated error ± 10%). [e] Fluorescence too low to be determined.

Table 2. Absorption and Steady-State Emission Properties of Representative Derivatives **3b** and **3k** in Various Solvents[a]

	3b				**3k**			
solvent[b]	λ_{abs}	log ϵ	λ_{em}	$\varphi_f \times 10^2$	λ_{abs}	log ϵ	λ_{em}	$\varphi_f \times 10^2$
H_2O	404	4.33	535	36	397	4.33	550	0.08
MeOH	404	4.40	534	40	400	4.36	542	0.05
MeCN	404	4.40	537	43	397	4.36	536	0.06
DMSO	406	4.37	546	41	402	4.33	552	0.18
CH_2Cl_2	409	4.40	526	59	413	4.29	527	0.59
	458	4.13						
$CHCl_3$	404	4.41	538	53	403	4.28	531	1.40
	449	4.13						

[a] See footnotes to Table 1. [b] In order of their decreasing E_T values.[56]

could not be detected (**3e**, **3f**). The fluorescence intensity of most of the aryl-substituted derivatives is slightly enhanced in chloroform solutions, reaching $\varphi_f = 0.014$ in the case of **3k**. If detectable, the emission spectrum of these compounds is usually broad and centered at $\lambda_{em} \approx 520-540$ nm, similar to the emission spectra of the brightly fluorescent dialkylamino derivatives **3a**−**c**. However, in the solid state or in colloid solutions (e.g., in ethyl acetate) compounds **3g**−**k** show a moderately intensive, orange emission with a broad maximum centered at around 600 nm (Figure S1B).

The absorption and emission properties of the derivative **3d**, which carries a conjugated dimethylamino group, change significantly upon protonation. The photometric titrations of hydrochloric acid to this compound in the Britton−Robinson buffer (an aqueous buffer solution consisting of phosphoric, boric, and acetic acids and providing a smooth pH change in a broad range, $1 \le pH \le 8$)[25] reveal the presence of several isosbestic points (Figure 2A). However, when **3d** was titrated with trifluoroacetic acid (TFA) in dichloromethane, the long-wavelength isosbestic points were not conserved during the titration (Figure 2B). Remarkably, the position and intensity of the long-wavelength absorption band (around 400 nm) do not change essentially during titration, while the other part of the

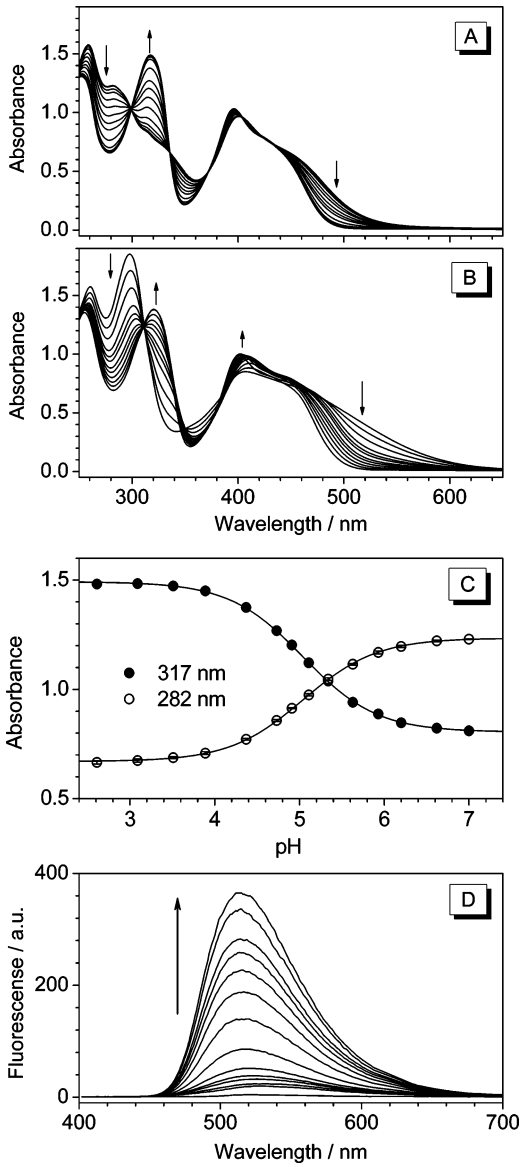

Figure 2. (A and B) Spectrophotometric titrations of compound **3d** (50 μM) with HCl in the Britton−Robinson buffer (A) and with TFA in dichloromethane (B). (C) Titration curves for the titration depicted in (A); numerical fits calculated for $K_a = 9.1 \times 10^{-6}$ M. (D) Spectrofluorimetric titration of TFA to **3d** (10 μM in dichloromethane). Arrows indicate changes in the intensities of bands upon acidification.

spectrum undergoes significant changes; that is, the long-wavelength tail of the absorption spectrum disappears, and a new band located at 320 nm arises. The titration curves may be fitted by the 1:1 protolytic equilibrium (Figure 2C); they give the values of acidity constants (pK_a, at 293 K) of 5.04 (in water) and 4.05 (in dichloromethane, fits not shown). In the fluorescence spectra of **3d**, the emission maxima remain essentially unchanged during the acid titration, but the fluorescence intensities increase. This effect is especially large when this compound is titrated with TFA in dichloromethane (Figure 2D). In this case the fluorescence intensity increases by a factor of ca. 130, and the emission maximum shifts by 11 nm to shorter wavelengths. In the other solvents, such as water and DMSO, the fluorescence enhancement is not as pronounced (cf. the φ_f values for the protonated and basic forms of **3d** in Table S1, Supporting Information).

(24) Reichardt, C. *Solvents and Solvent Effects in Organic Chemistry*, 3rd ed.; Wiley−VCH: Weinheim, 2003.
(25) Britton, H. T. S.; Robinson, R. A. *J. Chem. Soc.* **1931**, 458−473.

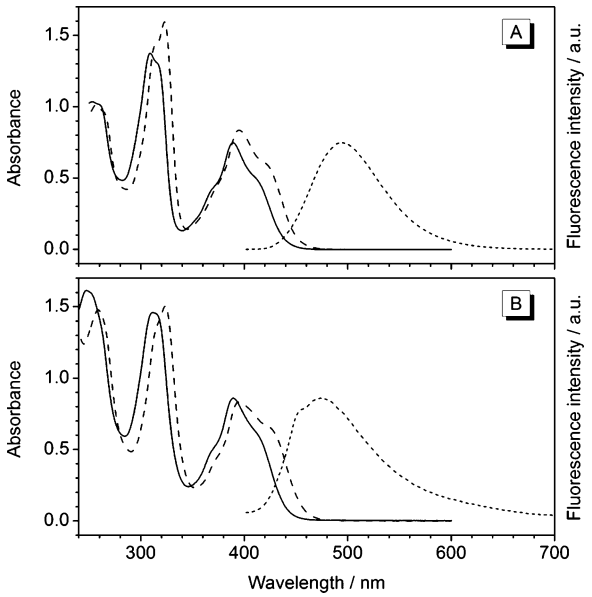

Figure 3. Absorption and fluorescence spectra of compounds **3m** (A) and **3l** (B). Solid lines: absorption spectra in water; dashed lines: absorption spectra in dichloromethane, $c = 50$ μM in both cases. Dotted lines: normalized fluorescence emission spectra in water, $c = 10$ μM, excitation wavelength $\lambda_{exc} = 390$ nm.

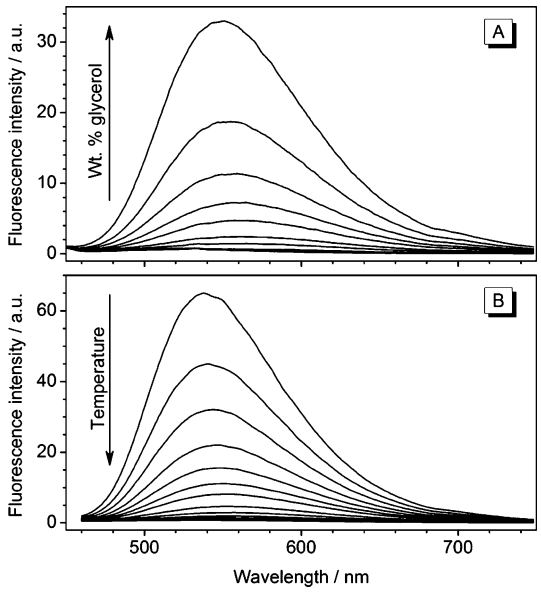

Figure 4. Fluorescence emission spectra of compound **3f** (A) in water−glycerol mixtures at 20 °C, the arrow indicates changes in fluorescence intensity upon increasing the glycerol content from 0 to 100%; (B) in glycerol at varied temperatures, the arrow indicates the changes in the intensity with increasing temperature. For the experimental conditions, see footnote to Table 3.

B. Absorption and Fluorescence Properties of 9-Sulfanyl-substitued Derivatives. The sulfanyl-substituted acridizinium derivatives **3l** and **3m** show absorption and fluorescence spectra (Figure 3) that are very similar to each other (cf. $\lambda_{max} = 390$ and 389 nm for **3l** and **3m** in water) and to the one of 9-aminoacridizinium (**1**; $\lambda_{max} = 387$ nm in water). The long-wavelength absorption bands of these compounds are slightly more structured than the ones of the amino-substituted analogues, and three constituents may be identified. The solvatochromism of these compounds is also negligible; thus, the absorption maxima of both compounds shift up to 395 nm (in dichloromethane).

The fluorescence spectra of compound **3m** have a maximum at 490−500 nm and are thus blue-shifted by about 40 nm compared to the *N*,*N*-dialkylamino derivatives **3a**−**c**. The Stokes shift (80−110 nm, depending on the solvent) is large but slightly smaller than the one observed for the amino-substituted analogues. The fluorescence quantum yields are about 0.20 in most solvents and thus are slightly smaller than the ones of compound **1** and *N*,*N*-dialkyl-substituted 9-aminoacridizinium salts **3a**−**b** ($\varphi_f \approx 0.4$ in water). In contrast to the amino analogues, such as **1** and **3a**−**c**, the fluorescence of compound **3m** is efficiently quenched in DMSO ($\varphi_f \approx 0.01$).

Compared to compound **3m**, the phenylsulfanyl-substituted derivative **3l** shows a much weaker fluorescence in all solvents investigated ($\varphi_f \leq 3 \times 10^{-3}$). Similarly to the *N*-aryl-substituted derivatives **3d**−**k**, the most intense fluorescence is observed in chloroform. The emission maximum of **3l** is located at 470−480 nm in most solvents, whereas in chloroform it undergoes a significant bathochromic shift up to $\lambda_{em} = 524$ nm.

C. Viscosity Dependence of the Fluorescence of the Aryl-Substituted Derivatives. To investigate the mechanism of the radiationless deactivation in the weakly fluorescent aryl-substituted derivatives **3d**−**k** and **3l**, the dependence of their fluorescence properties on the viscosity of the medium was studied. The latter was systematically varied by two methods: (i) solvents of different viscosity were used at a constant temperature, and (ii) a solvent whose viscosity changes to a large extent with the temperature was employed at varied temperatures.

The media of varied viscosity were provided by glycerol−water mixtures, since the latter allow investigations in a very broad range of viscosities (from $\eta = 1.005$ cP in water to 1499 cP in glycerol at 20.0 °C). The viscosity dependence of such mixtures on their content is well-documented.[26] Moreover, both glycerol and water are protic solvents with a comparable polarity ($E_T(30) = 63.1$ and 57.0 for water and glycerol, respectively),[24] allowing exclusion of influential factors other than viscosity on the fluorescence. The fluorescence of solutions of the aryl-substituted derivatives in such mixtures increases drastically with increasing glycerol content. The representative fluorescence spectra of the derivative **3g** in water−glycerol mixtures are shown in Figure 4A; similar changes were observed in the case of all other aryl-substituted derivatives, including compound **3l**. The values of fluorescence quantum yields in glycerol at 20 °C, as well as results of the linear regression analysis of the double-logarithmic plot of φ_f vs η, are summarized in Table 3.

In the case of the methoxy-substituted compound (**3e**), the fluorescence is enhanced by a factor of 25 upon a change from water to glycerol. This enhancement is even more pronounced in the case of derivatives **3f**−**i** and **3l** (increase by a factor of 60−130) and especially for the chloro-substituted compounds **3j** and **3k** (increase by a factor of 200 for both derivatives).

The effect of the temperature on the fluorescence properties was investigated for the solutions of several representative compounds in glycerol. Upon heating from 0 to 100 °C, the viscosity of this solvent decreases nonlinearly from 12 070 to 14.8 cP.[26] This causes a marked decrease of the fluorescence

(26) Andrussow, L.; Schram B. In *Eigenschaften der Materie in Ihren Aggregatzuständen: Transportphänomene I (Landolt-Börnstein, Bd. 5a)*; Schäfer, K., Ed.; Springer: Berlin, 1969; pp 371−373.

Table 3. Fluorescence Quantum Yields of Selected Acridizinium Derivatives in Glycerol and Results of the Linear Regression Analysis of log φ_f over log η[a]

				regression of log φ_f over log η	
compound	substituent	φ_f (glycerol)	φ_f (glycerol)/ φ_f (water)	slope k	r^2
3e	NH(4-C_6H_4OMe)	2.2×10^{-3}	25	0.45	0.998
3f	NH(4-C_6H_4Me)	8.5×10^{-3}	63	0.59	0.997
3g	NHPh	1.6×10^{-2}	110	0.65	0.996
3h	NH(4-C_6H_4F)	1.6×10^{-2}	130	0.69	0.996
3i	NH(4-C_6H_4Br)	1.7×10^{-2}	105	0.66	0.991
3j	NH(4-C_6H_4Cl)	3.1×10^{-2}	200	0.77	0.991
3k	NH(3-C_6H_4Cl)	7.1×10^{-2}	205	0.76	0.991
3l	SPh	3.3×10^{-2}	85	0.63	0.997

[a] Experimental conditions: temperature $\theta = 20.0$ °C; concentration $c = 10$ μM; excitation wavelength $\lambda_{ex} = 390$ nm in all cases. Fluorescence quantum yields determined with Coumarin 153 as a reference.

intensity of the aryl-substituted acridizinium derivatives (Figure 4B; see Figure S2 in the Supporting Information for the spectra of other derivatives). At the same time, the positions of the emission maximum change by 16−19 nm; thus, the emission spectra are most red-shifted at temperatures 50−60 °C, whereas at lower and at higher temperatures the emission maxima are shifted to the shorter wavelengths. Remarkably, the fluorescence quantum yield of compound **3j** in glycerol reaches the value 0.17 at 0 °C, and the yellow fluorescence of this compound may be observed by the naked eye.

Interaction of 9-Substituted Acridizinium Derivatives with DNA. A. Spectrophotometric Titrations. The interaction of the representative derivatives **3a**, **3b**, **3d**, **3e**, **3i**−**k**, and **3m** with DNA was investigated by spectrophotometric and spectrofluorimetric titrations with calf thymus DNA (ct DNA) in aqueous phosphate buffer solutions at pH 7.0. Spectrophotometric titrations of ct DNA to derivatives **3b** and **3j** and the sulfanyl analogue **3m** are shown in Figure 5 (see Figure S3, Supporting Information, for the titrations of the other derivatives). Upon addition of DNA to the buffered solutions of the acridizinium derivatives, a significant decrease of the absorbance (hypochromic effect) and a red shift (11−15 nm) of the long-wavelength absorption maxima were observed. Simultaneously new weak shoulders at longer wavelengths and one or more isosbestic points were detected, indicative of an interaction of the acridizinium derivative with DNA. Photometric titrations of DNA to the halogen-substituted derivatives **3i**−**j** at a dye concentration of 50 μM turned out to be problematic, since, at the beginning of the titrations, i.e., at high ligand-to-DNA ratios ($r > 0.25$), the colored, fibrous DNA−dye complex precipitated from the solution. Nevertheless, upon further addition of DNA ($r \leq 0.16$) the precipitate partly dissolved. For the evaluation of the DNA-binding constants and binding-site sizes, the data from spectrophotometric titrations were represented as Scatchard plots (Figure S4) and fitted to the neighbor-exclusion model of McGhee and von Hippel.[27]

The binding constants of the investigated compounds are in the 10^4 M^{-1} range within experimental error (Table 4). Compound **3b** has the largest value of $K = 4.4 \times 10^5$ M^{-1}. In general, the binding-site sizes for the dialkylamino-substituted derivatives **3a**−**b** and the methylsulfanyl derivative **3m** are larger than the values for the *N*-aryl derivatives ($n = 1.2-1.5$), which may be explained by the assumption that the latter compounds, in addition to the intercalation, at high ligand-to-DNA ratios form aggregates which stack along the DNA backbone. The binding of the compounds from the former subgroup is more consistent with the pure intercalative mode.

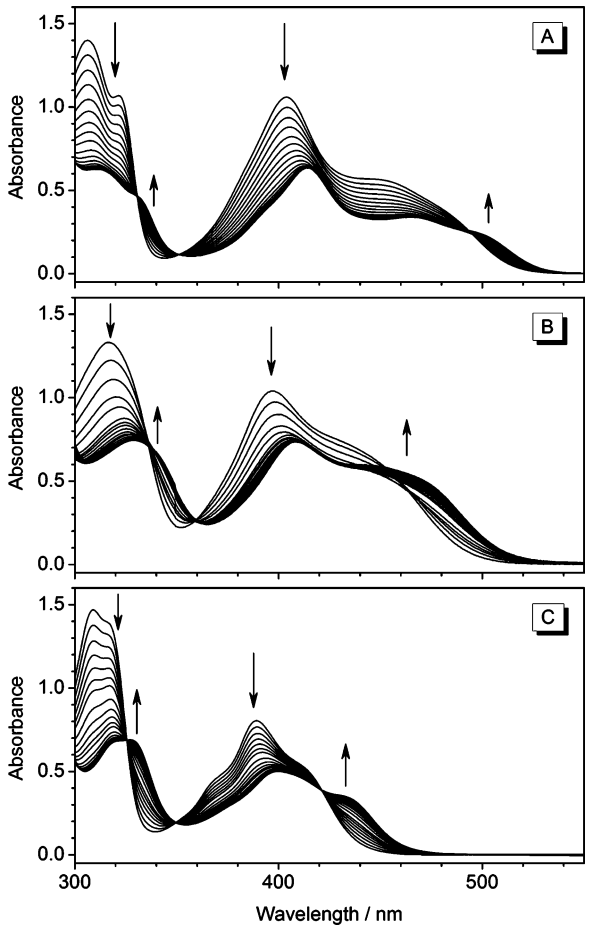

Figure 5. Spectrophotometric titrations of ct DNA to compounds **3b** (A), **3j** (B), and **3m** (C) at a dye concentration of 50 μM. The arrows indicate the changes of the intensity of the absorption bands upon addition of the DNA (0−0.5 mm).

B. Linear Dichroism Spectroscopy. Linear dichroism (LD) spectroscopy is an efficient tool to evaluate the binding modes between ligands and nucleic acids, based on the forced orientation of nucleic acid molecules in an external hydrodynamic (so-called *flow LD*) or electric field.[28] To determine the binding geometry of 9-substituted acridizinium derivatives, the flow LD

(27) McGhee, J. D.; von Hippel, P. H. *J. Mol. Biol.* **1974**, *86*, 469−489.

(28) (a) Nordén, B.; Kubista, M.; Kurucsev, T. *Quart. Rev. Biophys.* **1992**, *25*, 51−170. (b) Nordén, B.; Kurucsev, T. *J. Mol. Recognit.* **1994**, *7*, 141−156.

Table 4. DNA-Binding Properties of Selected Acridizinium Derivatives from Spectrophotometric and Fluorimetric Titrations

	λ_{abs}/nm[a]			λ_{em}/nm[b]				
	free	bound	shift $\Delta\lambda$	free	bound	shift $\Delta\lambda$	K[c]/10^4 M^{-1}	n[d]
3a	396	407	11	529	534	5	4.7 ± 0.2	2.4 ± 0.1
3b	404	415	11	537	540	3	44 ± 4	1.7 ± 0.1
3d	401	413	12	524	532	8	14 ± 1	1.5 ± 0.1
3e	398	413	15	519	519	0	6.8 ± 0.4	1.5 ± 0.1
3i	398	410	12	508	558	50	6.3 ± 0.4	1.2 ± 0.1
3j	397	409	12	513	555	42	5.8 ± 0.2	1.4 ± 0.1
3k	397	407	10	542	539	−3	*e*	*e*
3m	389	400	11	496	492	−4	7.5 ± 0.6	3.7 ± 0.1

[a] Absorption wavelengths that correspond to the free and bound dye absorption maxima, as well as the shift upon complex formation with DNA. [b] Emission maxima for the free and bound dye and the shift upon complex formation with DNA. [c] Binding constant (in bp), determined from fitting the Scatchard plots to the McGhee−von Hippel model. [d] Binding-site size (in bp), determined from fitting the Scatchard plots to the McGhee−von Hippel model. [e] Not determined due to precipitation of DNA−dye complex during titration.

spectra of two representative derivatives **3a** and **3j** were measured at varied ligand-to-DNA ratios ($r = 0.04$, 0.08, and 0.2). The LD signals of both compounds (Figure 6) are negative at all mixing ratios both in the UV region where both the DNA bases and the ligands absorb (<300 nm) and at wavelengths longer than 350 nm where only ligands absorb. Such negative LD bands are indicative of an intercalative mode of binding.

The reduced linear dichroism (LD_r) spectra provide information about the average orientation of the ligand transitions relative to the DNA base transitions. Typically, LD_r spectra are structureless, except in the regions of overlap of transitions with different polarizations, i.e., when different binding modes take place simultaneously. In the case of derivative **3a**, an essentially constant LD_r value between 350 and 500 nm, comparable to the one of the DNA bases (at 280 nm), indicates that a single binding mode, namely intercalation into the DNA, takes place. In contrast, for compound **3j**, the values of LD_r are slightly smaller than the ones of free DNA, which indicates a certain degree of tilting of the transition moment of the dye, and thus of the aromatic plane of the acridizinium chromophore, relative to the plane of the base pairs. From eq S14 (Supporting Information) it can be estimated that the transition dipole moment of the compound **3j** is tilted by 10°−20° relative to the orientation perpendicular to the helix axis. At higher ligand-to-DNA ratios ($r > 0.08$), the magnitude of the LD_r signal decreases due to the nonspecific association of the dyes on the DNA surface with a random orientation.

C. Spectrofluorimetric Titrations. Spectrofluorimetric titrations of ct DNA to the acridizinium derivatives **3a**−**b**, **3e**, **3i**−**k**, and **3m** were performed in an aqueous buffer solution at a ligand concentration of 10 μM. At these conditions, no precipitation was observed. Since the interaction with DNA also leads to significant changes in the absorption spectra of the dyes, the excitation wavelengths for the fluorimetric titrations corresponded to the isosbestic points, which were determined from the spectrophotometric titrations. The changes in the fluorescence emission spectra upon titration of ct DNA to selected derivatives are presented in Figure 7 and Figure 9A; the plots of the relative change of fluorescence intensity upon addition of DNA are shown in Figure 8.

The changes of the fluorescence properties of these compounds upon DNA addition show little regularities. Thus, the

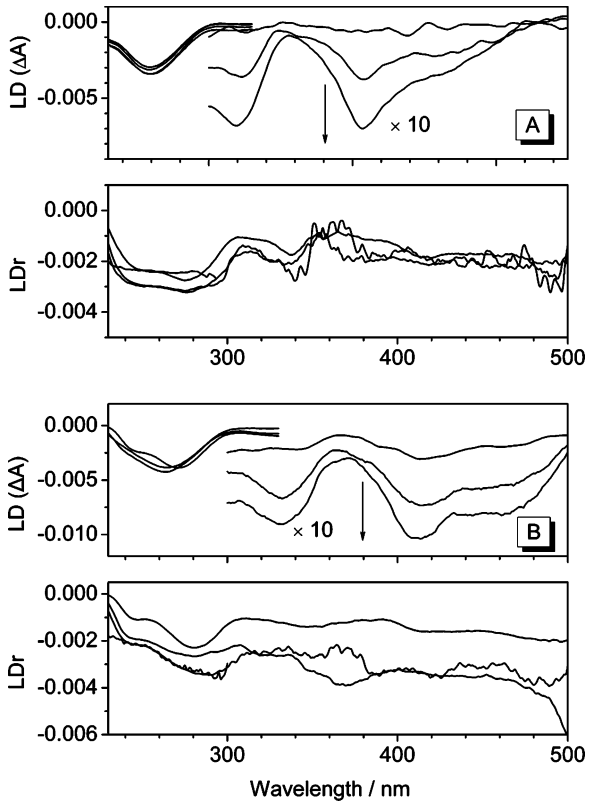

Figure 6. Linear dichroism (upper panels) and reduced LD (lower panels) spectra of compounds **3a** (A) and **3j** (B) in the presence of ct DNA. Arrows indicate the changes in the intensity of the bands with increasing ligand-to-DNA ratios ($r = 0.04$, 0.08, and 0.2).

dialkyl-substituted compounds **3a** and **3b** show opposite changes of their—intrinsically high—fluorescence properties. Compound **3a** shows a weak decrease of the fluorescence intensity similar to that of the parent compound **1**, while the fluorescence of **3b** slightly increases (Figure 7A). The emission maximum shifts to longer wavelengths in both cases, although the shift is small (5 and 3 nm, respectively).

Upon addition of ct DNA to the methoxy derivative **3e**, its weak intrinsic fluorescence decreases even further (Figure 7B). In the case of the bromo-substituted derivative **3i**, the fluorescence intensity increases by a factor of about 2.3 but remains rather low; at the same time, the emission maximum shifts by 50 nm to longer wavelengths, and an isoemissive point at $\lambda = 508$ nm is observed. The DNA-induced fluorescence enhancement is most pronounced in the case of the chloro-substituted derivatives **3j**−**k** (Figure 7C). The very weak fluorescence of these compounds in aqueous solutions increases by factors of approximately 30 and 50, respectively, upon addition of ct DNA (Figure 8). In the case of derivative **3j**, the emission maximum upon complex formation with DNA is considerably red-shifted with respect to the emission of the unbound compound (555 vs 513 nm). However, for the derivative **3k**, an opposite behavior is observed; thus, the emission maximum undergoes a small hypsochromic shift (539 vs 542 nm).

Upon titration of ct DNA to the solutions of the sulfanyl derivative **3m**, a marked decrease of the fluorescence intensity is observed, whereas the position of the emission band does not change significantly (Figure 9A). The quenching of the fluorescence in this case obeys the Stern−Volmer relationship

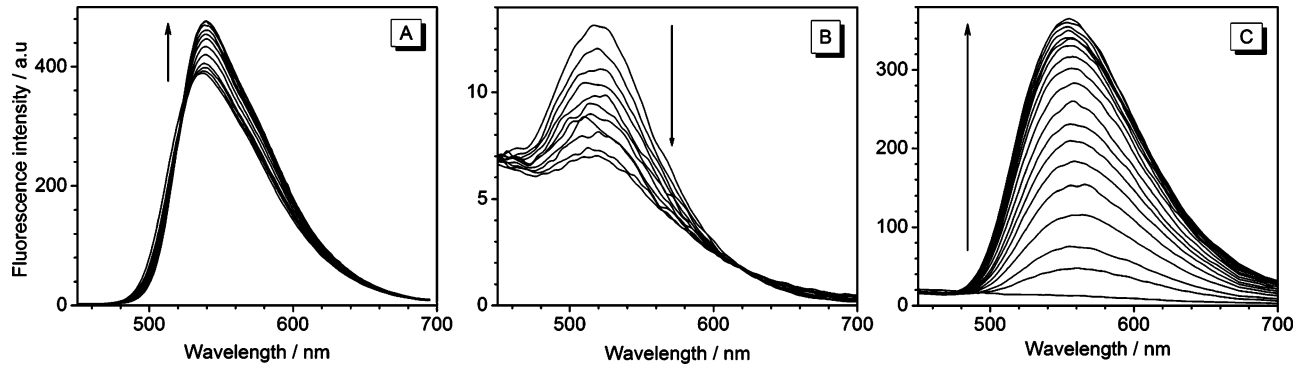

Figure 7. Spectrofluorimetric titrations of ct DNA to acridizinium derivatives **3b** (A, $\lambda_{ex} = 351$ nm), **3e** (B, $\lambda_{ex} = 362$ nm), and **3j** (C, $\lambda_{ex} = 336$ nm). Ligand concentration $c = 10$ μM in all cases. Arrows indicate changes in the fluorescence intensity during the titration.

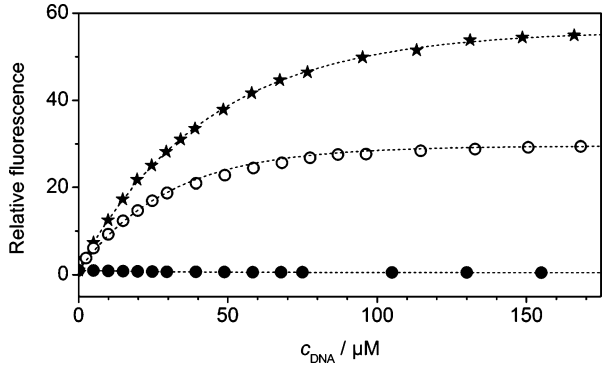

Figure 8. Changes of fluorescence intensity upon titration of ct DNA to the derivatives **3e** (●), **3j** (○), and **3k** (★).

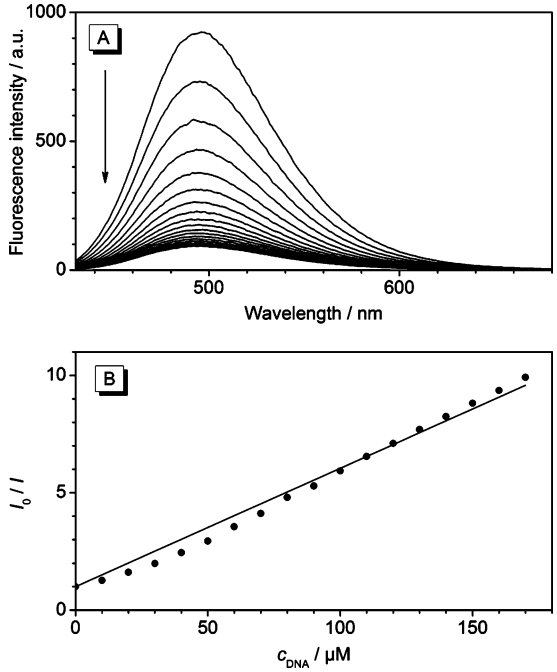

Figure 9. (A) Spectrofluorimetric titration of ct DNA to the derivative **3m** ($c = 10$ μM, $\lambda_{ex} = 421$ nm); the arrow indicates changes of fluorescence intensity during the titration. (B) Stern−Volmer plot for the titration.

(Figure 9B; $r^2 = 0.986$), and the quenching constant was determined to be $K_{SV} = 5.1 \times 10^4$ M^{-1} (bp).

Interaction of *N*-Aryl-9-aminoacridizinium Derivatives with Proteins. The interaction of the halogen-substituted compounds **3h** and **3j**−**k** with selected proteins, namely, bovine serum albumin (BSA), human serum albumin (HSA), and chicken egg white albumin (CEA), was studied by spectrophotometric and spectrofluorimetric titrations. Upon titration of these proteins to the aforementioned acridizinium derivatives in aqueous buffer solutions, no significant changes in the absorption spectra of the dyes were observed. However, in most cases an increase of the fluorescence intensity was detected. It was further observed that, like in the case of some proprietary fluorescent protein probes,[29] the anionic surfactant (SDS) shows a cooperative effect on the protein-induced fluorescence enhancement; therefore, in a preliminary experiment, an optimal concentration of SDS was determined. Thus, a solution of the dye **3k** (10 μM) in the presence of excess protein (500 μg mL^{-1} BSA) was titrated with a stock solution of SDS, and fluorescence spectra were recorded. The concentration of SDS, which induced the most intensive fluorescence signal, was 0.05% w/v (Figure S5, Supporting Information); at lower and at higher surfactant concentrations, a decrease of the fluorescence was observed. Therefore, all further fluorimetric titrations of proteins were performed in the presence of 0.05% SDS. It should be noted that, in the absence of proteins, SDS slowly induces the aggregation of the dyes, which causes changes in the fluorescence spectra and irreproducibility of the titrations. Therefore, aliquots of the SDS solution were added to the dye solutions directly before each titration experiment.

A representative spectrofluorimetric titration of BSA to compound **3k** in the presence of SDS is shown in Figure S5B (Supporting Information); the titration curves for the titration of various proteins to different halogen-substituted *N*-aryl-9-aminoacridizinium derivatives are shown in Figure 10. Remarkably, all investigated compounds show very similar behaviors upon binding to the proteins. Thus, the binding reaches saturation at protein concentrations of 600−800 μg mL^{-1}; at this point, the relative increase of the fluorescence constitutes a factor of about 20 for all compounds, although the *absolute* fluorescence intensities for these dyes are different. The observed difference between various proteins is also minor; thus, of the proteins investigated, BSA induced the steepest increase of fluorescence. It should be noted that the concentrations of the protein solutions used in these titrations were determined by the conventional Bradford assay, which is known to have some protein-to-protein variability,[29] and this may cause some

(29) Jones, L. J.; Haugland, R. P.; Singer, V. L. *BioTechniques* **2003**, *34*, 850−861.

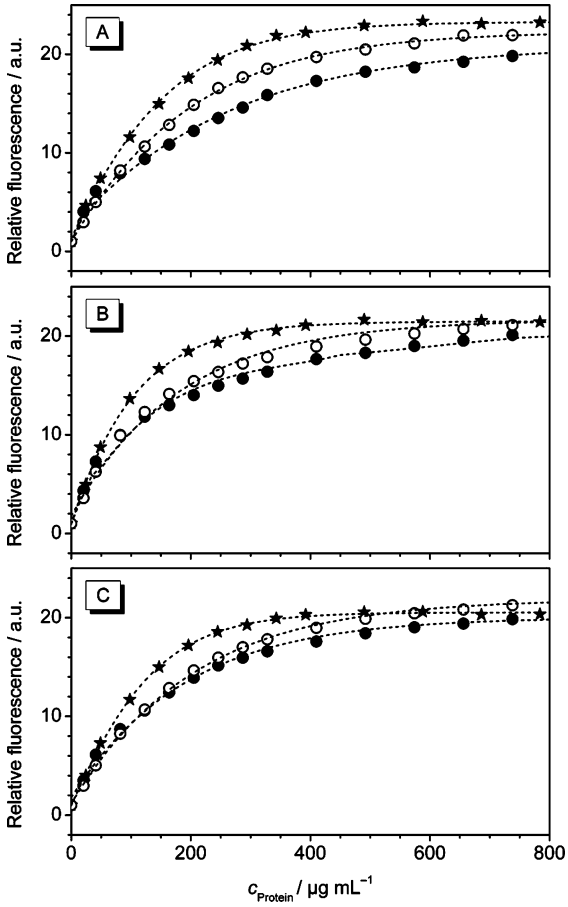

Figure 10. Titration curves for the spectrofluorimetric titrations of proteins [(●) HSA, (○) CEA, (★) BSA] to derivatives **3h** (A), **3j** (B), and **3k** (C); c(**3**) = 10 μM in BPE buffer with 0.05% SDS; excitation wavelength λ_{ex} = 397 nm in all cases.

deviations in the actual titration curves. Remarkably, at low protein concentrations (0−50 μg mL^{-1}), the relationship between the fluorescence intensity of the dyes and the protein concentration is linear, as determined by the fluorimetric titrations with diluted protein solutions (Figure S6, Supporting Information).

Discussion

Photophysical Properties of 9-Substituted Acridizinium Derivatives. With respect to the emission properties, the series of the 9-substituted acridizinium derivatives investigated in this work may be divided into two groups: (i) the parent compound **1**,[18] its *N*,*N*-dialkyl-substituted derivatives **3a**−**c**, and the sulfanyl analogue **3m** show significant fluorescence properties with moderate to large quantum yields (φ_f = 0.2−0.6, depending on the solvent); (ii) the *N*-aryl derivatives **3d**−**k** and the sulfanyl analogue **3l** exhibit essentially no or very weak fluorescence in solution ($\varphi_f \leq 0.01$). However, despite these substantial differences in the fluorescence properties, the position and the shape of the long-wavelength band ($S_0 \rightarrow S_1$ transition) in the absorption spectra of the compounds from both groups are similar ($\lambda_{max} \approx$ 390−410 nm). Moreover, the fluorescence emission spectra of the compounds from the second group—in the cases when an unambiguous detection was possible—are located in the same wavelength region as the ones of the compounds from the second group ($\lambda_{em} \approx$ 510−550 nm).

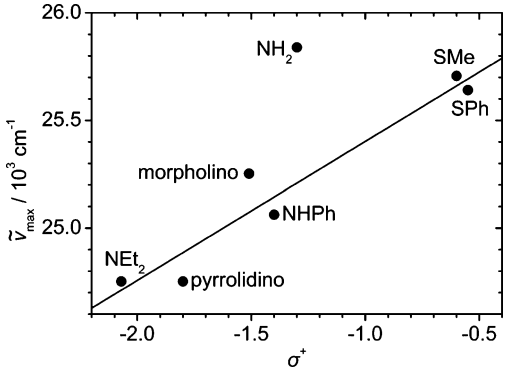

Figure 11. Correlation between the energy of the long-wavelength transition in 9-substituted acridizinium derivatives (in water) and the Hammett−Brown substituent parameter σ^+.

Scheme 1. Donor−Acceptor Interplay in the 9-Donor-Substituted Acridizinium Derivatives

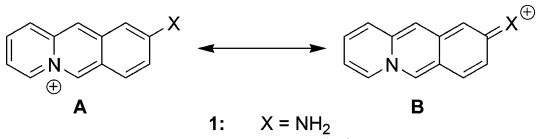

A. First Group: Derivatives with Intensive Intrinsic Fluorescence. The photophysical properties of the 9-aminoacridizinium **1**, i.e., large red shift of the absorption compared to the unsubstituted acridizinium chromophore and a remarkably large Stokes shift of the fluorescence ($\Delta\lambda \approx$ 120 nm), may be rationalized on the basis of two resonance forms **A** and **B** (Scheme 1).[18] Thus, in the ground state, canonical structure **A** may be more favored, whereas the first excited state is better represented by structure **B**. The energy difference between these canonical forms determines the absorption shift, as has been demonstrated for cyanine dyes.[30]

This scheme may be applied also to the derivatives **3a**−**c** and **3m**. Thus, the introduction of a stronger electron donor instead of the amino group in **1**, e.g., morpholino (**3a**) or pyrrolidino (**3b**) residues, results in the bathochromic shifts of the $S_0 \rightarrow S_1$ transition by 9 nm (590 cm^{-1}) for **3a** and by 17 nm (1090 cm^{-1}) for **3b** (the data refer to solutions in water, if not stated otherwise). These results are in accordance with the observations that morpholino and especially pyrrolidino substituents are stronger electron donors than the unsubstituted amino group.[31] A quantitative treatment of these data shows a good correlation (r^2 = 0.93 upon exclusion of compound **1**) between the energy of the $S_0 \rightarrow S_1$ transition and the Hammett−Brown substituent parameter σ^+ (Figure 11).[32] The use of the σ^+ parameter (which has been determined for the heterocyclic substituents only recently)[32b] is reasonable because it appropriately represents the π-donating properties of the substituents in conjugated systems.

(30) (a) Fabian, J.; Hartmann, H. *Light Absorption of Organic Colorants*; Springer: Berlin, 1980. (b) Ischenko, A. A. *Structure and Luminescent Spectral Properties of Polymethine Dyes*; Naukova Dumka: Kiev, 1994 (in Russian).
(31) (a) Effenberger, F.; Fischer, P.; Schoeller, W. W.; Stohrer, W.-D. *Tetrahedron* **1978**, *34*, 2409−2417. (b) Firl, J.; Braun, H.; Amann, A.; Barnett, R. *Z. Naturforsch.* **1980**, *35b*, 1406−1414.
(32) (a) Hansch, C.; Leo, C.; Taft, R. W. *Chem. Rev.* **1991**, *91*, 165−195. (b) Mayr, H.; Bug, T.; Gotta, M. F.; Hering, N.; Irrgang, B.; Janker, B.; Kempf, B.; Loos, R.; Ofial, A. R.; Remennikov, G.; Schimmel, H. *J. Am. Chem. Soc.* **2001**, *123*, 9500−9512.

It should be noted that the data for the 9-aminoacridizinium **1** deviate significantly from the trend, presumably due to specific interactions of the protons of the amino group with the solvent, which influence the apparent electron-donor properties of the substituent. Thus, it has been shown that the position of the absorption band of **1** in protic solvents undergoes a hypsochromic shift, which correlates with the acceptor number, i.e., the electron-acceptor properties of the solvent, indicating the formation of the hydrogen bonds.[18] Therefore, the unsubstituted amino functionality is not an appropriate benchmark to compare electron-donating properties. This explains why the replacement with the methylsulfanyl substituent in compound **3m**, i.e., a weaker donor than the amino group, results in a small bathochromic shift (2 nm, 130 cm^{-1}) as compared to that for compound **1**.

Remarkably, the shifts of absorption maxima, resulting from the replacement of the amino group with other substituents, are lower than those in other donor−acceptor dyes. Thus, it has been shown that in the related *N*-substituted 7-amino-1-methylquinolinium salts replacement of the amino group with a morpholine residue results in a bathochromic shift by 1090 cm^{-1}, whereas the introduction of an alkylsulfanyl group causes a hypsochromic shift by 850 cm^{-1}.[33] Even a more pronounced effect has been observed in the cationic styrylpyridinium dyes; i.e., the replacement of the amino group with a pyrrolidine residue results in a bathochromic shift by ~1600 cm^{-1}.[34]

The minor solvatochromic properties of the 9-donor-substituted acridizinium derivatives may be rationalized assuming a similar polarity of the ground and first excited states of the chromophore. Thus, these compounds, along with the quinolinium analogues,[33] represent the so-called *charge-resonance* chromophores of the $D-\pi-A^+$ X^- architecture, which, in contrast to the *charge-transfer* chromophores of the $D-\pi-A$ type, are relatively insensitive to the polarity of the medium. The solvatochromism usually arises from different stabilizations of the ground and excited states of the chromophore by the solvent; however, since both structures **A** and **B** (Scheme 1) are charged species, there is no significant difference in the stabilization.[24] However, it was observed that in dichloromethane solutions a significant red shift of the absorption maxima, a blue shift of the emission maxima, and an increase of the fluorescence quantum yield for these derivatives take place (cf. Table 2). This observation may be attributed to the high polarizability of this solvent ($\alpha = 6.52$ Å^3),[35] since it facilitates the fast redistribution of the polarizable electrons during excitation. Thus, after the vertical excitation upon photon absorption, the initially formed excited Franck−Condon (FC) state propagates to the solvent-relaxed FC state, followed by the geometrical relaxation to the vibrationally relaxed S_1 state (for a diagram that sketches the discussed mechanism and the relative energy levels, see Supporting Information, Figure S7).[1e] From the latter state the fluorescence and nonradiative processes usually occur at room temperature. In the case of a highly polarizable solvent the vertical electronic excitation is accompanied by an instant rearrangement of the electrons of the solvent cage, leading directly to the solvent-relaxed excited FC state and decreasing the energy of the excited state. This leads to a bathochromic shift of absorption. In the case of fluorescence emission, the same mechanism takes place and lowers the apparent energy of the ground FC state, as the fluorescence is accompanied by repolarization of the solvent cage and finishes at the solvent-relaxed S_0−FC state. This results in an increase of the energy of the radiative $S_1 \rightarrow S_0$ transition (hypsochromic shift). Such anomalous shifts of absorption and fluorescence bands and an increase of fluorescence quantum yield in dichloromethane have been occasionally observed for cationic dyes[33,36] but are rarely addressed in the literature, as these effects are usually masked by the more pronounced polarity-dependent solvatochromic shifts and become evident only in the case of polarity-independent charge resonance dyes. Interestingly, chloroform ($\alpha = 8.53$ Å^3) does not cause a similar effect in this subseries, although it is observed in the *N*-aryl derivatives **3d**−**k**.

The reduced fluorescence quantum yield of the sulfanyl-substituted derivative **3m** ($\varphi_f = 0.15-0.20$), as compared to the amino analogues **3a**−**c** ($\varphi_f = 0.20-0.60$), may be attributed to the enhanced intersystem crossing rate in **3m** due to the presence of the sulfur atom in the chromophore (internal heavy-atom effect).[37] A similar decrease of the fluorescence quantum yield has been observed for the sulfur derivatives of charge-resonance dyes.[33] The exceptional decrease of fluorescence of **3m** in DMSO is presumably due to the higher reduction potential of this chromophore compared to the amino analogues, in combination with the high electronic donor strength of the solvent. A similar quenching in DMSO has also been observed for the unsubstituted acridizinium cation.[38] Moreover, this assumption is supported by the efficient fluorescence quenching of **3m** by the DNA (cf. Figure 9).

B. Second Group: Derivatives with Low Intrinsic Fluorescence. All *N*-aryl-9-aminoacridizinium salts **3d**−**k** possess much weaker intrinsic fluorescence than the parent compound **1** and the above-discussed derivatives. At the same time, the absorption spectra of these derivatives, with the exception of the 4-(dimethylamino)phenylamino derivative **3d**, closely resemble each other and the spectra of dialkyl-substituted derivatives **3a**−**c**. Moreover, the position of the absorption maximum of the *N*-phenyl-substituted derivative **3g** correlates well with the σ^+ parameter for the phenylamino group (Figure 11). The fluorescence bands of these derivatives, in spite of their low intensity, also lay in the same region as the ones of the derivatives **3a**−**c**. These observations may be rationalized by the assumption that, in the ground state, the aryl substituents do not interact with the chromophore, which is formed by the 9-aminoacridizinium residue per se. Instead, in the ground state, the phenyl ring is oriented almost perpendicular relative to the plane of the aminoacridizinium chromophore, similarly to the orientation in 2-*N*-arylamino-6-naphthalenesulfonate derivatives **13**.[39] Further support of this hypothesis comes from the analysis of the protolytic equilibria in compound **3d**.

(33) van den Berg, O.; Jager, W. F.; Picken, S. J. *J. Org. Chem.* **2006**, *71*, 2666−2676.
(34) Gawinecki, R.; Trzebiatowska, K. *Dyes Pigm.* **2000**, *45*, 103−107.
(35) Bosque, R.; Sales, J. *J. Chem. Inf. Comput. Sci.* **2002**, *42*, 1154−1163.
(36) (a) Horng, M. L.; Dahl, K.; Jones, G. II; Maroncelli, *M. Chem. Phys. Lett.* **1999**, *315*, 363−370. (b) Jager, W. F.; Kudasheva, D.; Neckers, D. C. *Macromolecules* **1996**, *29*, 7351−7355.
(37) Nijegorodov, N.; Mabbs, R. *Spectrochim. Acta, Part A* **2001**, *57*, 1449−1462.
(38) Bendig, J.; Helm, S.; Kreysig, D.; Wilda, J. *J. Prakt. Chem.* **1982**, *324*, 978−986.
(39) (a) Kosower, E. M. *Acc. Chem. Res.* **1982**, *15*, 259−266. (b) Kosower, E. M.; Dodiuk, H.; Tanizawa, K.; Ottolenghi, M.; Orbach, N. *J. Am. Chem. Soc.* **1975**, *97*, 2167−2178. (c) Dodiuk, H.; Kosower, E. M. *J. Phys. Chem.* **1977**, *81*, 50−54. (d) Kosower, E. M.; Dodiuk, H. *J. Phys. Chem.* **1978**, *82*, 2012−2015.

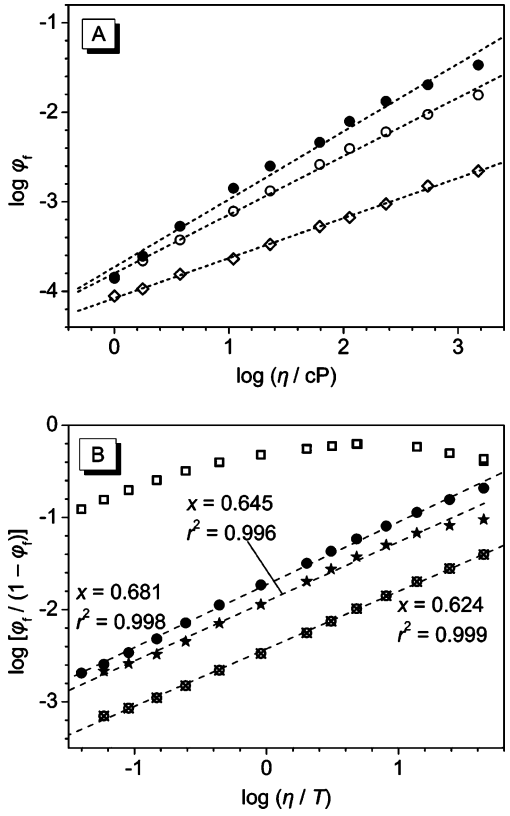

Figure 12. (A) Viscosity dependence of fluorescence quantum yields for compounds **3e** (◇), **3g** (○), and **3j** (●), measured in water−glycerol mixtures. (B) Plot of $\log[\varphi_f/(1-\varphi_f)]$ vs $\log(\eta/T)$ for compounds **3c** (□), **3f** (⊗), **3j** (●), and **3l** (★) in glycerol; *x*, slopes of the linear fits.

Compound **3d** with a 4-dimethylamino substituent in the phenyl ring shows a very broad absorption band extending up to 600 nm. Since the shape of the absorption spectrum remains essentially unchanged in a broad concentration range (Figure S2, Supporting Information), the formation of aggregates may be excluded as a possible reason for such band broadening. On the other hand, the long-wavelength part of this band decreases upon acidification (Figure 2A and B). This observation indicates that the long-wavelength absorption is due to a pronounced excited-state electron transfer between the *para*-aminophenyl substituent and the acridizinium chromophore, which disappears as the electron-donating properties of the dimethylamino functionality are suppressed by the protonation. The observed value of the acidity constant in water ($pK_a = 5.04$ at 293 K) is very close to the one of *N*,*N*-dimethylaniline ($pK_a = 5.15$ at 298 K)[40] but significantly larger than the ones of donor−acceptor systems, such as 4-dimethylamino-4′-cyanobiphenyl ($pK_a = 2.35$ in EtOH−water)[41] or 9-[(4-dimethylamino)phenyl]-10-methylacridinium perchlorate ($pK_a = 3.38$ in water).[42] These data indicate that the 9-aminoacridizinium chromophore *as a whole* acts as a very weak electron acceptor and has no mesomeric effect on the attached aryl substituent.

While the unprotonated form of **3d** is virtually nonfluorescent, the protonated form exhibits a weak fluorescence with an emission centered at about 510−530 nm (Table 1; Figure 2C). This phenomenon is more pronounced in dichloromethane and chloroform solutions, most likely due to the high polarizability of these solvents.

C. Deactivation Pathways. The fluorescence quantum yield of *N*-aryl-9-aminoacridizinium salts **3d**−**k** increases drastically with increasing rigidity of the medium, either by using solvent mixtures with increasing viscosity or upon decreasing the temperature. A similar behavior has been observed for a large number of dyes that undergo a conformational change in the excited state, such as di- and triphenylmethane dyes,[43] phenyl-substituted heterocycles,[44] and donor−acceptor systems that form a twisted intramolecular charge transfer (TICT) state, in which the orbitals of the donor and acceptor constituents are perpendicular.[45,46] The ANS derivatives **13** also belong to the latter group.[39] However, in certain donor−acceptor systems the intramolecular charge transfer takes place from an almost planar geometry.[47]

Since it was demonstrated that the fluorescence emission of the *N*-aryl derivatives **3d**−**k** originates from the 9-aminoacridizinium chromophore, the possibility of the rotation about the acridizinium C9−N bond may be excluded as the deactivation pathway. Moreover, the fluorescence of the parent compound **1**,[48] as well as of *N*,*N*-dialkylsubstituted derivatives, such as **3c**, does not show any significant viscosity dependence (Figure 12B). Therefore, it may be proposed that a radiationless deactivation of the excited state in **3d**−**k** is due to the excited-state rotation about the N−C(phenyl) bond.

It has been shown that in the solutions of medium-to-high viscosity the internal rotation (torsional relaxation) of the probe molecules is controlled by the free-volume effects rather than by the bulk viscosity of the solutions.[1e] Thus, an empirical relationship (eq 1) between the fluorescence quantum yield, φ_f, of fluorophores which may undergo torsional relaxation and viscosity of the medium η has been proposed (eq 1).[1e,49]

$$\frac{\varphi_f}{1-\varphi_f} = a(\eta/T)^x \qquad (1)$$

This relationship holds under assumptions that the intrinsic radiative lifetime of the excited state is independent of the temperature T and viscosity η. Usually, $x < 1$ and emphasizes the influence of the effective viscosity of the medium, which is less than the bulk viscosity because of the free-volume effects. Under conditions of constant temperature and small fluorescence quantum yields ($\varphi_f \ll 1$), eq 1 may be simplified to the Förster−Hoffmann equation (eq 2), which reveals the power dependence

(40) Dean, J. A., Ed. *Lange's Handbook of Chemistry*, 14th ed.; McGraw-Hill: New York, 1992.
(41) Maus, M.; Rurack, K. *New J. Chem.* **2000**, *24*, 677−686.
(42) Jonker, S. A.; Ariese, F.; Verhoeven, J. W. *Recl. Trav. Chim. Pays-Bas* **1989**, *108*, 109−115.
(43) (a) Oster, G.; Nishijima, Y. *J. Am. Chem. Soc.* **1956**, *78*, 1581−1584. (b) Förster, T.; Hoffmann, G. *Z. physik. Chem. NF* **1971**, *75*, 63−76. (c) Vogel, M.; Rettig, W. *Ber. Bunsenges. Phys. Chem.* **1985**, *89*, 962−968. (d) Gautam, P.; Harriman, A. *J. Chem. Soc., Faraday Trans.* **1994**, *90*, 697−701.
(44) Belletête, M.; Sarpal, R. S.; Durocher, G. *Chem. Phys. Lett.* **1993**, *201*, 145−152.
(45) Grabowski, Z. R.; Rotkiewicz, K.; Rettig, W. *Chem. Rev.* **2003**, *103*, 3899−4031.
(46) (a) Loutfy, R. O.; Arnold, B. A. *J. Phys. Chem.* **1982**, *86*, 4205−4211. (b) Rettig, W. *J. Phys. Chem.* **1982**, *86*, 1970−1976. (c) Wandelt, B.; Turkewitch, P.; Stranix, B. R.; Darling, G. D. *J. Chem. Soc., Faraday Trans.* **1995**, *91*, 4199−4205. (d) Demeter, A.; Bérces, T.; Biszók, L.; Wintgens, V.; Valat, P.; Kossanyi, J. *J. Phys. Chem.* **1996**, *100*, 2001−2011. (e) Bon Hoa, G. H.; Kossanyi, J.; Demeter, A.; Biszók, L.; Bérces, T. *Photochem. Photobiol. Sci.* **2004**, *3*, 473−482.
(47) Yoshihara, T.; Druzhinin, S. I.; Zachariasse, K. A. *J. Am. Chem. Soc.* **2004**, *126*, 8535−8539.
(48) Otto, D. Dissertation, Universität Siegen, 2007.
(49) Adam, W.; Matsumoto, M.; Trofimov, A. V. *J. Am. Chem. Soc.* **2000**, *122*, 8631−8634.

of the fluorescence quantum yield on the viscosity of the solution.[43b]

$$\varphi_f = C\eta^k \quad (2)$$

The dependence of fluorescence quantum yields of selected *N*-aryl-9-aminoacridizinium derivatives on the viscosity of the medium, provided by water−glycerol mixtures at a constant temperature, is presented in Figure 12A. An almost linear fit in the double-logarithmic coordinates may be observed for all aryl-substituted derivatives (Table 3). This behavior is in good agreement with the Förster−Hoffman equation. Moreover, the results show that the *k* values for the *N*-phenyl derivative **3g** and for the derivatives with weak electron-acceptor substituents (F, Br) in the phenyl group are very close to the value of $k = {}^2/_3$, which has been theoretically derived by Förster and Hoffmann for the rotation of the phenyl group and which has been found for the triphenylmethane dyes and many similar systems, e.g., 2-phenylindolenine.[44]

The results of the fluorescence measurements of selected compounds (**3f** and **3j**) in glycerol solutions at varied temperatures were treated according to the more exact eq 2. The results (Figure 12B) show a linear dependence of $\varphi_f/(1 - \varphi_f)$ on (η/T) in the double-logarithmic coordinates. Moreover, the values of the exponent ($x = 0.62-0.68$) are in good agreement with the values found from the experiments at a constant temperature and with the ones reported for the other systems with a phenyl group that may undergo a torsional reorientation.[1e] Therefore, it may be concluded that one of the main excited-state deactivation pathways includes the rotation of the phenyl group, most likely accompanied by the simultaneous elongation of the N−C(phenyl) bond.

The data in Table 3 also show that the derivatives with an electron-donor substituent in the phenyl ring have lower *k* values than *N*-phenyl-9-aminoacridizinium **3g** and the derivatives with electron-acceptor substituents. Thus, $k = 0.45$ and 0.59 were found for the derivatives **3e** (R = OMe) and **3f** (R = Me), respectively, while the derivatives with the electron-acceptor chloro substituents (**3j**−**k**) have larger *k* values (0.76−0.77) than the compound **3g** ($k = 0.65$). Moreover, the values of the fluorescence quantum yield of the derivatives **3e**−**k** in glycerol solutions, i.e., under conditions when the rotational relaxation of the excited state is impeded, are not equal but show an apparent dependence on the electron-donating strength of the substituent, as characterized by the substituent constant (Figure 13).

Therefore, it may be proposed that there exists another radiationless pathway for the deactivation of the excited state, the efficiency of which is dependent on the electron density on the phenyl ring that is provided by the substituent. Similarly to the ANS system **2**, it may be concluded that this pathway is represented by an excited-state electron transfer from the phenyl group to the photoexcited 9-aminoacridizinium chromophore (Figure 14A). The validity of the proposed mechanism may be demonstrated by the protolytic viscosity dependence of fluorescence of derivative **3d** (Figure 14B). Thus, the unprotonated form of **3d** is virtually nonfluorescent either in aqueous solutions or at the conditions of increased viscosity (glycerol solutions), where the rotational deactivation pathway is suppressed. The protonation of the dimethylamino group, which transforms it from the electron-donor to the electron-acceptor substituent and thereby blocks the electron-transfer deactivation pathway, does not lead to a significant increase of fluorescence at the low-viscosity conditions, i.e., in an aqueous solution. However, when the protonation is performed in a highly viscous glycerol solution, an intense green fluorescence may be observed, as both nonradiative deactivation pathways for the excited state are hindered. Therefore, the salt **3d** may be regarded as a molecular "logic gate" of the AND type[50] that transforms two different input parameters (proton concentration and the viscosity of the medium) into one output signal, namely fluorescence. Interestingly, although many examples of both viscosity-dependent[43,44] and the pH-sensitive[1] fluorescent probes are known, the combination of both input parameters in one molecule has not been described, to the best of our knowledge.

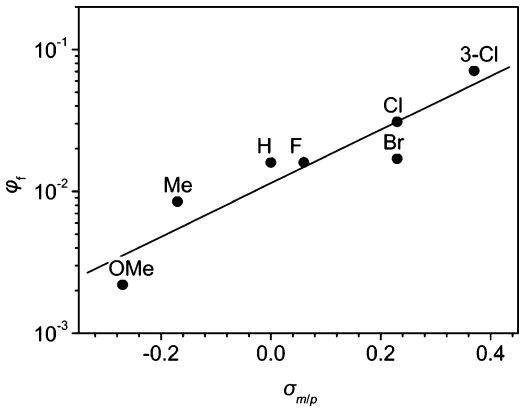

Figure 13. Dependence of the fluorescence quantum yield of derivatives **3e**−**k** in glycerol on the Hammett substituent constant σ.

D. Interaction of 9-Substituted Acridizinium Derivatives with DNA. The results of the spectrophotometric titrations of selected 9-substituted acridizinium derivatives with DNA, namely a significant hypsochromic effect of the long-wavelength absorption band and the formation of new red-shifted bands, indicate binding of these compounds to the DNA. The isosbestic points, observed in most cases, indicate that one binding mode takes place almost exclusively. An exception from this behavior was observed for the halogen-substituted derivatives **3i**−**k**, for which the long-wavelength isosbestic point was not conserved during the titration (Figure 5B), most likely due to the contribution of an additional binding mode at these ligand-to-DNA ratios. The linear dichroism spectroscopy of the dye−DNA complexes reveals that both compounds **3a** and **3j** intercalate into ds DNA, as indicated by the negative LD bands in the presence of DNA (Figure 10). The reduced LD spectrum provides further information on the average orientation of the transition moment of the chromophore relative to those of the DNA bases and allows distinguishing between homogeneous and heterogeneous binding. For the *N*,*N*-dialkylamino derivative **3a**, the LD_r spectrum is consistent with a coplanar orientation of the chromophore plane relative to the plane of the DNA bases, confirming intercalation, such as in the case of the parent compound **1**.[17] In contrast, the analysis of the LD_r spectrum of compound **3j** reveals a tilting of the acridizinium chromophore by about 10° relative to the DNA bases. This observation demonstrates that ionic interactions or groove binding also contribute to the overall binding of this compound to the DNA. This heterogeneous binding is confirmed by the loss of the

(50) Raymo, F. M. *Adv. Mater.* **2002**, *14*, 401−414.

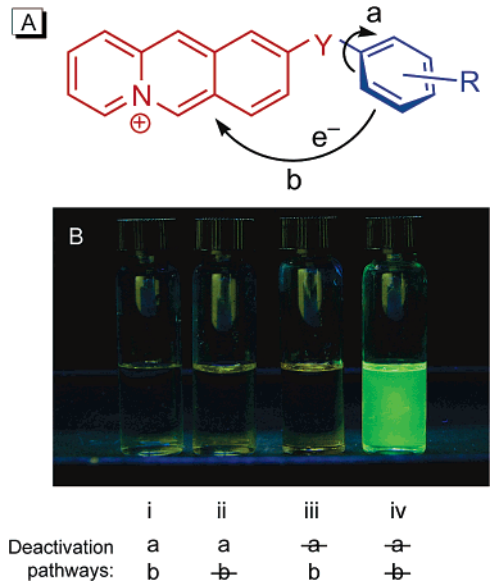

Figure 14. (A) Proposed model for the radiationless deactivation of the excited state in *N*-aryl-9-aminoacridizinium salts, including torsional relaxation of the phenyl group (a) and excited-state electron transfer (b). The chromophore unit is shown red. (B) Photograph of solutions of **3d** in water (i, pH 7), aq. HCl (ii, pH ≈ 1), glycerol (iii), and acidified (ca. 0.1 M HCl) glycerol (iv) under UV illumination (λ_L = 366 nm). Concentration c = 50 μM in all cases.

isosbestic point in the UV/vis titration. Thus, it may be estimated that dialkylamino-substituted derivatives **3a**−**b**, as well as the parent compound **1** and the sulfur analogue **3m**, bind to ds DNA exclusively by intercalation, whereas in the case of most *N*-aryl derivatives the intercalative binding mode prevails at low DNA-to-dye ratios, and at higher DNA concentrations another binding mode with a low binding constant takes place, which may be assigned to the assembly of the dye cations on the surface of DNA.

The interaction of the dyes **3a**−**k** with the DNA has an influence on their emission properties. While this influence is rather weak in the case of compounds **3a**−**b**, the derivatives **3i**−**k** with halogen substituents in the phenyl ring exhibit a remarkable fluorescence enhancement upon interaction with the DNA. This enhancement is rather weak for **3i** and significant in the case of **3j** and **3k** (by factors of 30 and 50). Apparently, the intercalation of the acridizinium chromophore into the DNA helix reduces the possibility of free rotation about the *N*−aryl bond, which prevents the nonradiative decay from the excited state. Compared to the derivative **3e**, which has a methoxy substituent in the phenyl ring, it may be assumed that in the latter case another deactivation pathway, namely the electron-transfer process from the electron-rich phenyl substituent to the acridizinium cation, prevents the fluorescence enhancement upon association with DNA. The smaller fluorescence enhancement of **3i** as compared to **3j**−**k** may be attributed to the internal heavy atom effect in **3i**. This asumption is supported by the observation that the fluorescence intensity of **3i** is also lower than the ones of the chloro-substituted derivatives in a highly viscous environment that suppresses the torsional relaxation pathway (cf. Table 3). A similar effect was found in the structurally similar ANS system.[39c]

These results indicate that, with an appropriate substitution pattern, *N*-aryl-9-amino-substituted acridizinium salts may be used as fluorescent "light-up" probes for DNA detection. Notably, the enhancement of fluorescence intensity of **3k** upon addition of DNA is larger than the ones observed for the conventional DNA stains, such as ethidium bromide ($I_{max}/I_0 \approx$ 10) and Hoechst 33258 ($I_{max}/I_0 \approx 30$),[7] so that this dye may be used complementary to the already established ones.

E. Interaction of *N*-Aryl-9-aminoacridizinium Derivatives with Proteins. The halogen-substituted derivatives **3h** and **3j**−**k** exhibit a significant fluorescence enhancement upon interaction with the proteins, such as human and bovine serum albumins and egg-white albumin. This fluorescence enhancement becomes more pronounced in the presence of an anionic surfactant (SDS), which is known to denaturate the proteins and form structures, in which the surfactant micelles are distributed along the unfolded protein molecules (necklace-and-beads model).[51] However, excess SDS leads to a decrease of the fluorescence, since the surfactant begins to displace the protein-bound probe molecules. A similar dependence of fluorescence on the surfactant concentration has been observed for other fluorescent probes, such as the ANS derivative TNS (**2b**)[51] and Nile Blue,[52] and has been used in some patented fluorescence-based assays for quantification of proteins in solution.[29] It may therefore be assumed that the role of SDS is the denaturation of the proteins, which provides access to the probe-binding sites which otherwise cannot be occupied by the dye molecules. Remarkably, the factors of the fluorescent enhancement for the different compounds investigated are essentially the same, which leads to the conclusion that these probes occupy the same, or at least very similar, binding sites. Such as in the case of the interaction with DNA, binding of the *N*-aryl-9-aminoacridizinium derivatives to the proteins reduces the conformational freedom of the probe molecule and leads to hindered rotation of the phenyl group and an increase of the fluorescence quantum yield.

The fluorescence enhancement upon interaction of compounds **3j**−**k** with proteins ($I_{max}/I_0 \approx 20$) is smaller than the one observed for TNS ($I_{max}/I_0 \approx 100$);[53] however, the fluorescence maximum of acridizinium derivatives are located at longer wavelengths (540 nm vs about 460 nm in the case of TNS) and thus more advantageous for the fluorimetric detection. It should be noted that recently a series of squaraine dyes for the fluorimetric detection of albumins has been described.[15a] Such dyes possess high sensitivity ($I_{max}/I_0 \approx 80$) and emit at long wavelengths ($\lambda_{em} \approx$ 610 nm), but their application in the presence of surfactants was not tested. Along these lines, *N*-aryl-9-amino-substituted acridizinium derivatives represent fluorescent probes which are consistent with the surfactants used in the protein gel electrophoresis and may find application for protein detection in gel electrophoresis due to the low protein-to-protein variability. Moreover, quantitative fluorimetric detection of the proteins in solution within this concentration range

(51) (a) Turro, N. J.; Lei, X.-G. *Langmuir* **1995**, *11*, 2525−2533. (b) Santos, S. F.; Zanette, D.; Fischer, H.; Itri, R. *J. Colloid Interface Sci.* **2003**, *262*, 400−408.
(52) Lee, S. H.; Suh, J. K.; Li, M. *Bull. Korean Chem. Soc.* **2003**, *24*, 45−48.
(53) Daniel, E.; Weber, G. *Biochemistry* **1966**, *5*, 1893−1900.
(54) (a) Loutfy, R. O. *Pure Appl. Chem.* **1986**, *58*, 1239−1248. (b) Bosch, P.; Catalina, F.; Corrales, T.; Peinado, C. *Chem.−Eur. J.* **2005**, *11*, 4314−4325.
(55) Haidekker, M. A.; Brady, T. P.; Lichlyter, D.; Theodorakis, E. A. *J. Am. Chem. Soc.* **2006**, *128*, 398−399.
(56) (a) Haidekker, M. A.; Ling, T.; Anglo, M.; Stevens, H. Y.; Frangos, J. A.; Theodorakis, E. A. *Chem. Biol.* **2001**, *8*, 123−131. (b) Haidekker, M. A.; Brady, T. P.; Chalian, S. H.; Akers, W.; Lichlyter, D.; Theodorakis, E. A. *Bioorg. Chem.* **2004**, *32*, 274−289.

may be achieved, provided a calibration curve had been constructed prior to the determination.

Conclusions

The nonradiative deactivation pathways of aryl-substituted 9-donor-acridizinium derivatives include an excited-state rotation of the phenyl group and, in the case of electron-donor substituents in the phenyl ring, an electron transfer from the phenyl ring to the electronically excited acridizinium chromophore. Therefore, these compounds represent fluorescence probes, almost insensitive to the changes in the *polarity* of the medium but with a pronounced susceptibility to the *rigidity* of the environment. Apart from the prospects for the detection of biomacromolecules, such as double-stranded DNA and proteins, the aforementioned properties may lead to applications of the *N*-aryl-9-aminoacridizinium derivatives in which the changes of the probe signal due to the changes in polarity are undesired, as they can obstruct the changes arising from other events, such as fluctuations in the rigidity of the medium. Such applications include, e.g., on-line monitoring of polymerization reactions and aging of polymers,[33,54] fluorimetric measurement of viscosity of liquids,[55] and measurement of microviscosity of the cell structures.[56]

Acknowledgment. This paper is dedicated to Prof. Waldemar Adam on the occasion of his 70th birthday. Generous financial support by the *Deutsche Forschungsgemeinschaft* is gratefully acknowledged.

Supporting Information Available: Experimental procedures, absorption and fluorescence emission data for all compounds, in various solvents, Scatchard plots for the determination of DNA-binding constants, graphs of the fluorimetric titrations of proteins, and a diagram that sketches the relative energies of a chromophore in the ground and excited state. This material is available free of charge via the Internet at http://pubs.acs.org.

JA0668872